

A KINEMATIC ANALYSIS OF TROPICAL STORM  
BASED ON ATS CLOUD MOTIONS

by

T. Theodore Fujita and Jaime J. Tecson



MESOMETEOROLOGY PROJECT --- RESEARCH PAPERS

- 1.\* Report on the Chicago Tornado of March 4, 1961 - Rodger A. Brown and Tetsuya Fujita
- 2.\* Index to the NSSP Surface Network - Tetsuya Fujita
- 3.\* Outline of a Technique for Precise Rectification of Satellite Cloud Photographs - Tetsuya Fujita
- 4.\* Horizontal Structure of Mountain Winds - Henry A. Brown
- 5.\* An Investigation of Developmental Processes of the Wake Depression Through Excess Pressure Analysis of Nocturnal Showers - Joseph L. Goldman
- 6.\* Precipitation in the 1960 Flagstaff Mesometeorological Network - Kenneth A. Styber
- 7.\*\* On a Method of Single- and Dual-Image Photogrammetry of Panoramic Aerial Photographs - Tetsuya Fujita
8. A Review of Researches on Analytical Mesometeorology - Tetsuya Fujita
- 9.\* Meteorological Interpretations of Convective Nephosystems Appearing in TIROS Cloud Photographs - Tetsuya Fujita, Toshimitsu Ushijima, William A. Hass, and George T. Dellert, Jr.
- 10.\* Study of the Development of Prefrontal Squall-Systems Using NSSP Network Data - Joseph L. Goldman
11. Analysis of Selected Aircraft Data from NSSP Operation, 1962 - Tetsuya Fujita
12. Study of a Long Condensation Trail Photographed by TIROS I - Toshimitsu Ushijima
13. A Technique for Precise Analysis of Satellite Data; Volume I - Photogrammetry (Published as MSL Report No. 14) - Tetsuya Fujita
14. Investigation of a Summer Jet Stream Using TIROS and Aerological Data - Kozo Ninomiya
15. Outline of a Theory and Examples for Precise Analysis of Satellite Radiation Data - Tetsuya Fujita
16. Preliminary Result of Analysis of the Cumulonimbus Cloud of April 21, 1961 - Tetsuya Fujita and James Arnold
17. A Technique for Precise Analysis of Satellite Photographs - Tetsuya Fujita
- 18.\* Evaluation of Limb Darkening from TIROS III Radiation Data - S.H.H. Larsen, Tetsuya Fujita, and W.L. Fletcher
19. Synoptic Interpretation of TIROS III Measurements of Infrared Radiation - Finn Pedersen and Tetsuya Fujita
- 20.\* TIROS III Measurements of Terrestrial Radiation and Reflected and Scattered Solar Radiation - S.H.H. Larsen, Tetsuya Fujita, and W.L. Fletcher
21. On the Low-level Structure of a Squall Line - Henry A. Brown
- 22.\* Thunderstorms and the Low-level Jet - William D. Bonner
- 23.\* The Mesoanalysis of an Organized Convective System - Henry A. Brown
24. Preliminary Radar and Photogrammetric Study of the Illinois Tornadoes of April 17 and 22, 1963 - Joseph L. Goldman and Tetsuya Fujita
25. Use of TIROS Pictures for Studies of the Internal Structure of Tropical Storms - Tetsuya Fujita with Rectified Pictures from TIROS I Orbit 125, R/O 128 - Toshimitsu Ushijima
26. An Experiment in the Determination of Geostrophic and Isallobaric Winds from NSSP Pressure Data - William Bonner
27. Proposed Mechanism of Hook Echo Formation - Tetsuya Fujita with a Preliminary Mesosynoptic Analysis of Tornado Cyclone Case of May 26, 1963 - Tetsuya Fujita and Robbi Stuhmer
28. The Decaying Stage of Hurricane Anna of July 1961 as Portrayed by TIROS Cloud Photographs and Infrared Radiation from the Top of the Storm - Tetsuya Fujita and James Arnold
29. A Technique for Precise Analysis of Satellite Data, Volume II - Radiation Analysis, Section 6. Fixed-Position Scanning - Tetsuya Fujita
30. Evaluation of Errors in the Graphical Rectification of Satellite Photographs - Tetsuya Fujita
31. Tables of Scan Nadir and Horizontal Angles - William D. Bonner
32. A Simplified Grid Technique for Determining Scan Lines Generated by the TIROS Scanning Radiometer - James E. Arnold
33. A Study of Cumulus Clouds over the Flagstaff Research Network with the Use of U-2 Photographs - Dorothy L. Bradbury and Tetsuya Fujita
34. The Scanning Printer and Its Application to Detailed Analysis of Satellite Radiation Data - Tetsuya Fujita
35. Synoptic Study of Cold Air Outbreak over the Mediterranean using Satellite Photographs and Radiation Data - Aasmund Rabbe and Tetsuya Fujita
36. Accurate Calibration of Doppler Winds for their use in the Computation of Mesoscale Wind Fields - Tetsuya Fujita
37. Proposed Operation of Instrumented Aircraft for Research on Moisture Fronts and Wake Depressions - Tetsuya Fujita and Dorothy L. Bradbury
38. Statistical and Kinematical Properties of the Low-level Jet Stream - William D. Bonner
39. The Illinois Tornadoes of 17 and 22 April 1963 - Joseph L. Goldman
40. Resolution of the Nimbus High Resolution Infrared Radiometer - Tetsuya Fujita and William R. Bandeen
41. On the Determination of the Exchange Coefficients in Convective Clouds - Rodger A. Brown

\* Out of Print

\*\* To be published

(Continued on back cover)

A KINEMATIC ANALYSIS OF TROPICAL STORM  
BASED ON ATS CLOUD MOTIONS

by

T. Theodore Fujita and Jaime J. Tecson  
Department of the Geophysical Sciences  
The University of Chicago

SMRP Research Paper No. 125

August 1974

This work was performed under the sponsorship of the U. S. Department of Commerce,  
National Oceanic and Atmospheric Administration, Grant No. 04-3-022-8.



# A KINEMATIC ANALYSIS OF TROPICAL STORM BASED ON ATS CLOUD MOTIONS

T. Theodore Fujita and Jaime J. Tecson  
Department of the Geophysical Sciences  
The University of Chicago

## ABSTRACT

An attempt is made to determine the asymmetric structure of an incipient storm in the Atlantic Ocean using low-cloud velocities computed from the Applications Technology Satellite (ATS III) picture sequences. The investigation concerns the kinematic analysis of tropical storm Anna during the three days on July 26, 27 and 28, 1969 when it has intensified into tropical storm stage in the vicinity of  $10^{\circ}$  N and  $35^{\circ}$  W reportedly late on the 27th.

It is found that the cross-equatorial flow from the southern hemisphere is mainly responsible for providing the inflow to the storm while the northern hemisphere trades supply the major contribution to the circulation around the storm. The inflow from the southern sector of the disturbance appears to increase, and so does the over-all circulation, as the storm intensifies.

## 1. INTRODUCTION

Cloud motion analysis from Applications Technology Satellite (ATS) photographs has been increasingly utilized in studying flow patterns in the atmosphere over various portions of the globe, especially over the tropics and temperate regions. With the advent of the similarly-designed Synchronous Meteorological Satellite (SMS), it is felt that this method of analysis will continue for some time. To a large extent, efforts are

being directed towards establishing some relationship between cloud motion and wind flow considering that tracer clouds provide ample supply of the necessary vectors to study horizontal circulation patterns. Statistical values and information on cloud distribution and motion, among others, are being compiled to serve as reference and guide. On the other hand, individual case studies are being carried out in order to probe into the individual characteristics of different nephosystems. Various techniques in tracing cloud motions have been employed by different investigators, among them, Serebreny et al. (1967), Fujita et al. (1968), Suomi et al. (1972), and Chang et al. (1973).

Tropical storms are readily one of the most common subjects of investigation using cloud motion analysis considering their influence in large-scale motion and the need to know more of their characteristics and behavior. From the velocity computations using the METRACOM system made by Chang and Tecson (1974) during the BOMEX Fourth Phase experiment in July 1969, an interesting case of the development of tropical storm Anna in the North Atlantic during the three-day period from July 26 through 28, 1969 in its incipient stage has been investigated. Agee (1972), in his study of the same storm through examination of ATS III photographs has presented a case of wave instability in the ITCZ, independent of easterly disturbances, which is responsible for tropical cyclone formation. He has indicated the contribution towards storm formation of the horizontal cyclonic wind shear present in the easterly flow, and has observed the absence of rotational development in the southern part of the wave.

This paper attempts a kinematic analysis of tropical storm Anna when it first intensified into a tropical storm based on ATS cloud motions.

## 2. BRIEF HISTORY OF TROPICAL STORM ANNA

For a more detailed account of tropical storm Anna, refer to the article by De Angelis (1970) and the North Atlantic Tropical Cyclone Track therewith. Only a brief history is presented below.

Tropical storm Anna, which had alternately intensified and weakened during its existence from July 23 to August 5, was the first tropical storm of 1969. Originating near the African continent, it became an organized depression on the 24th and attained tropical storm strength late on the 27th. On July 28, maximum winds reached 50 kts near  $13^{\circ}$  N and  $36^{\circ}$  W. Figure 1 shows the track of storm Anna. The positions for

July 26 through 28 are based on ATS cloud photographs. The translational speed averaged 10 kts toward the northwest. Unfortunately, there were no ATS pictures available on the 25th. In the absence of firm data, therefore, positions from July 24 to 25 are adjusted. The rest of the track is plotted following that from the North Atlantic Tropical Cyclone Track. Anna's movement from July 28 was generally northwesterly, recurving northeasterly late on August 2. It was a tropical storm from July 27 through July 31, 1969.

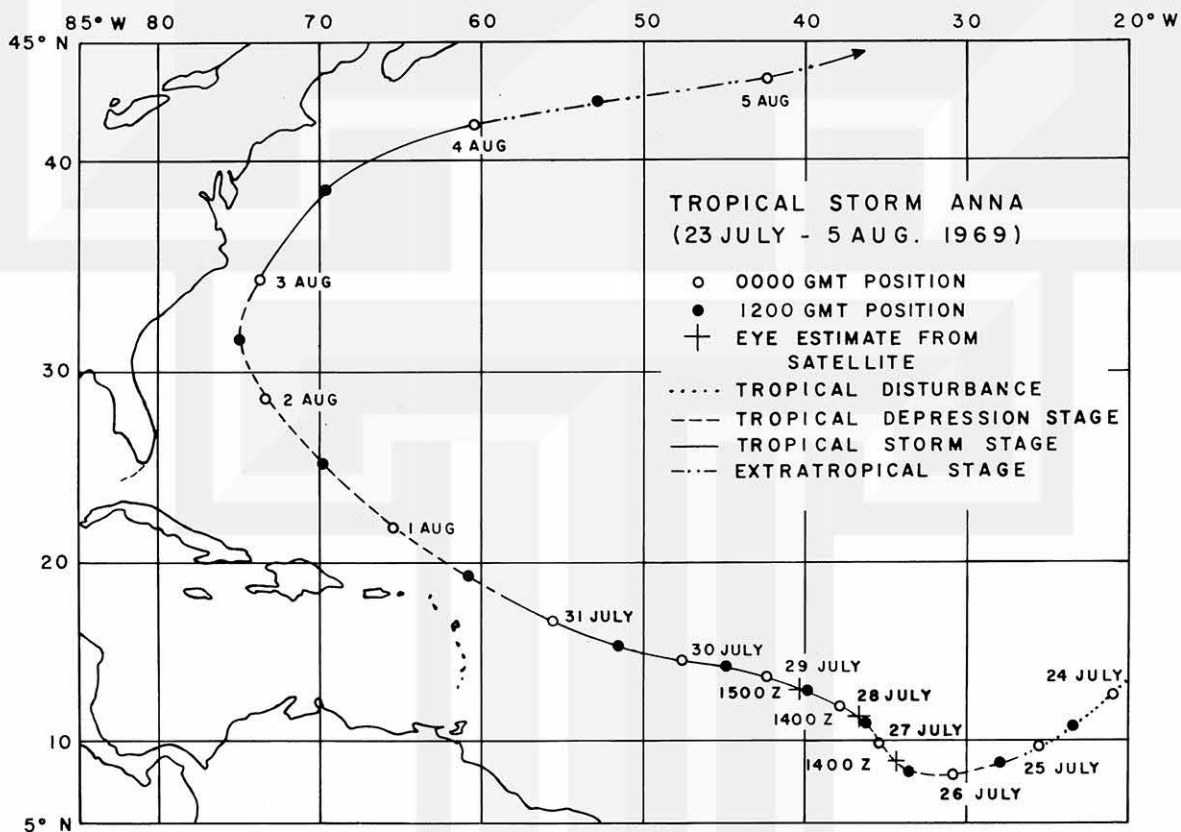


Fig. 1. Track of tropical storm Anna. The positions for July 26, 27 and 28, 1969 are estimated from ATS III cloud photographs. The rest of the track is plotted following that from the North Atlantic Tropical Cyclone Track, Climatological Data, National Summary, Annual 1969.

### 3. DATA USED AND METHOD OF ANALYSIS

ATS III photographs used as beginning frames in the movie computation loop for each day from July 26 through 28, 1969, are presented in Fig. 2. Actually, each movie loop is comprised of enlargement prints of the area within the rectangular box from which

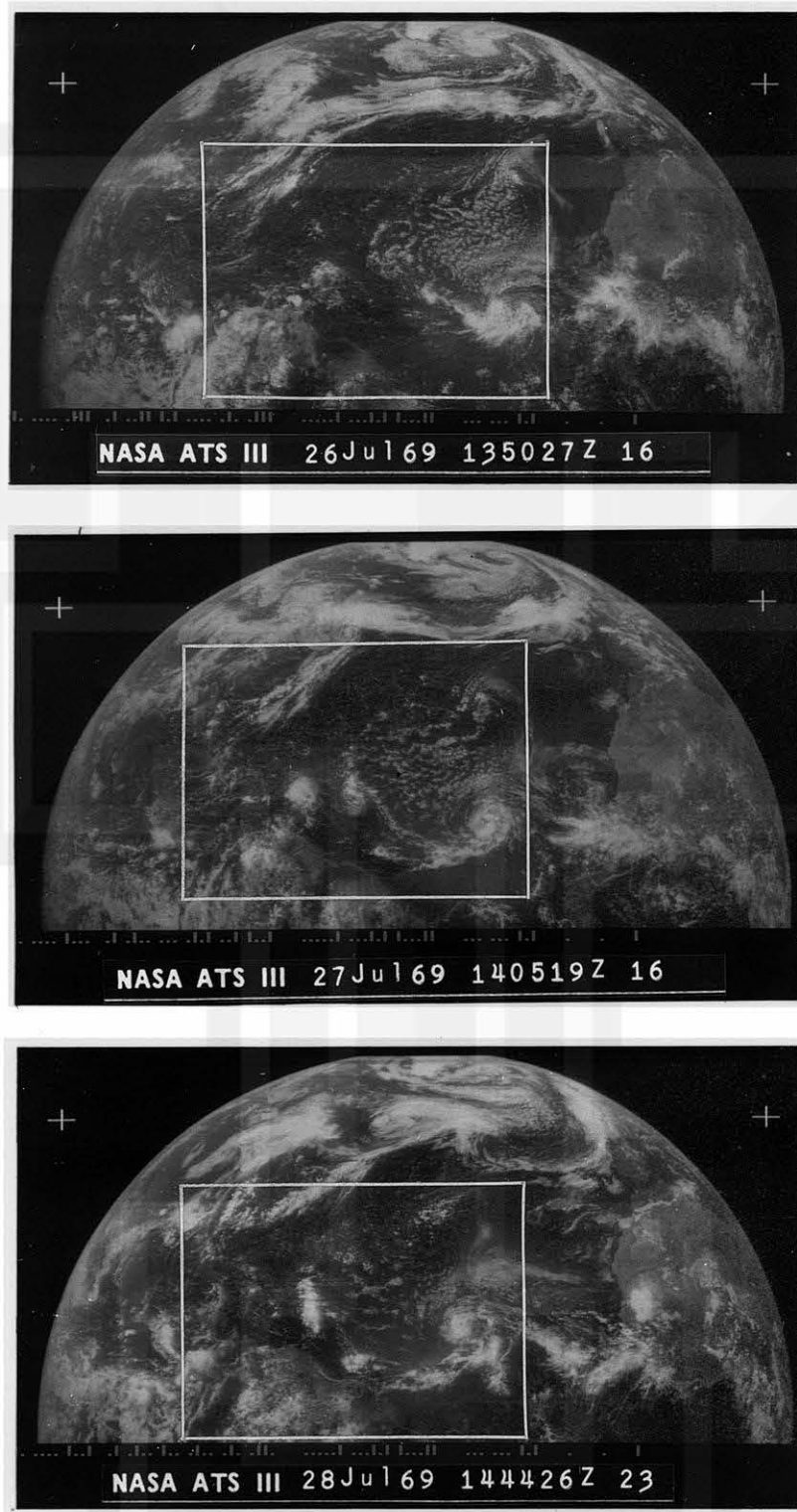


Fig. 2. ATS III global photographs comprising the beginning times of cloud velocity computation for each day from July 26 through 28, 1969. Rectangular boxes indicate areas analyzed.

the low-cloud velocities are computed. Figures 3, 4, and 5, reprinted from Chang and Tecson (1974), show the computed low-cloud velocity vectors and streamlines for July 26, 27 and 28, respectively, for the North Atlantic Ocean area east of the United States between  $0^{\circ}$  N to  $32^{\circ}$  N and  $30^{\circ}$  W to  $75^{\circ}$  W. Cloud configurations associated with storm Anna are seen at the lower right section of the charts. The time and period of computation are listed below:

Date (1969)	Period (Min.)	Mid-Time (GMT)
July 26	64	1422
July 27	74	1442
July 28	64	1516

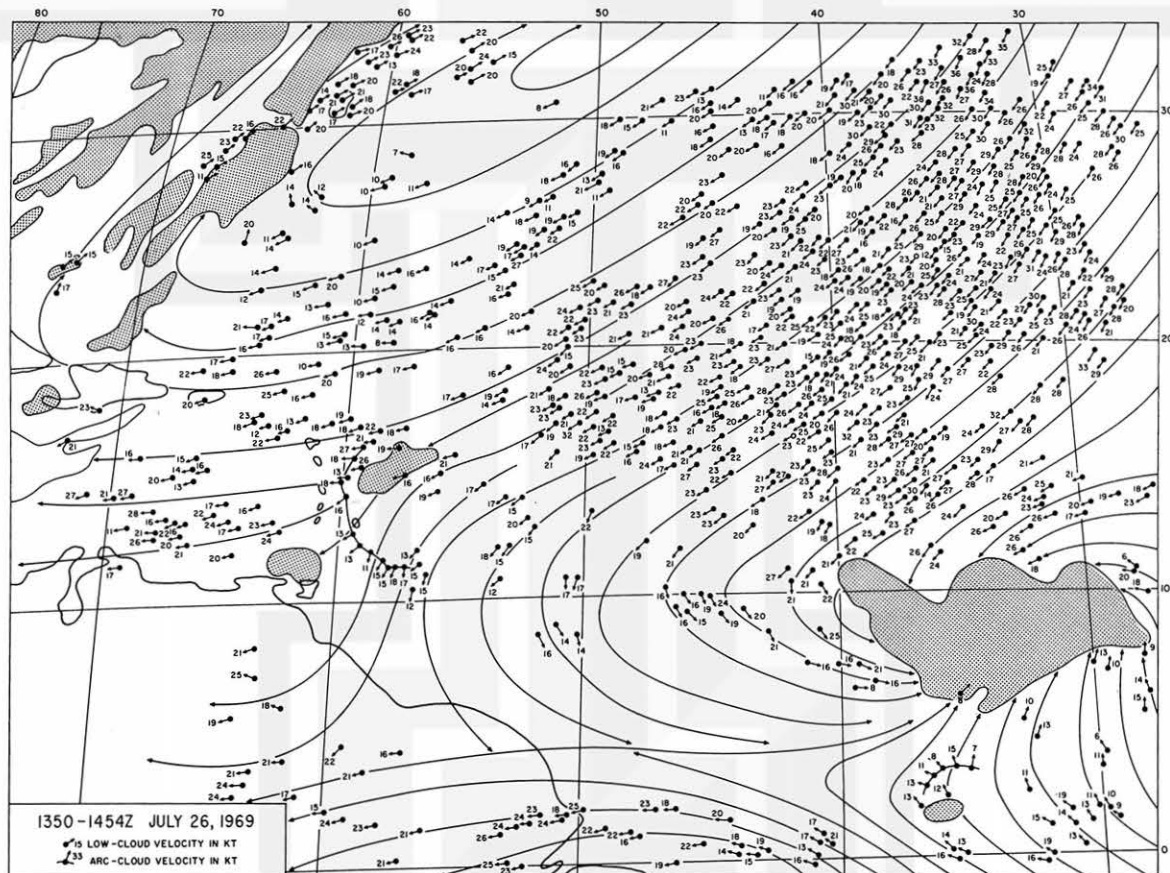


Fig. 3. Velocity vectors of low clouds for the analysis area in Fig. 2 on July 26, 1969 with superimposed streamlines. High clouds, shown as shaded areas, associated with developing storm Anna, are on the lower right section. (From Chang and Tecson, 1974.)

This indicates that the computation of the cloud velocities cover an average period of 67 minutes and that the time of computation for each day seems almost the same, say within an hour of each other. During this 3-day period, Anna has intensified from a tropical depression into a storm. Post analysis shows that it reached storm stage near 1200 Z on July 27.

Processing of the data consisted of computing the radial and tangential components of each cloud velocity vector, relative to a system of polar coordinates with the origin at the storm center. The angle from the radius vector to the cloud vector is measured. The components are then obtained. Total cloud velocities are computed in this case study, hence the asymmetry arising from superposition of vortex and steering current is preserved. It must be noted that only actual vectors are used; this lacks the smoothing

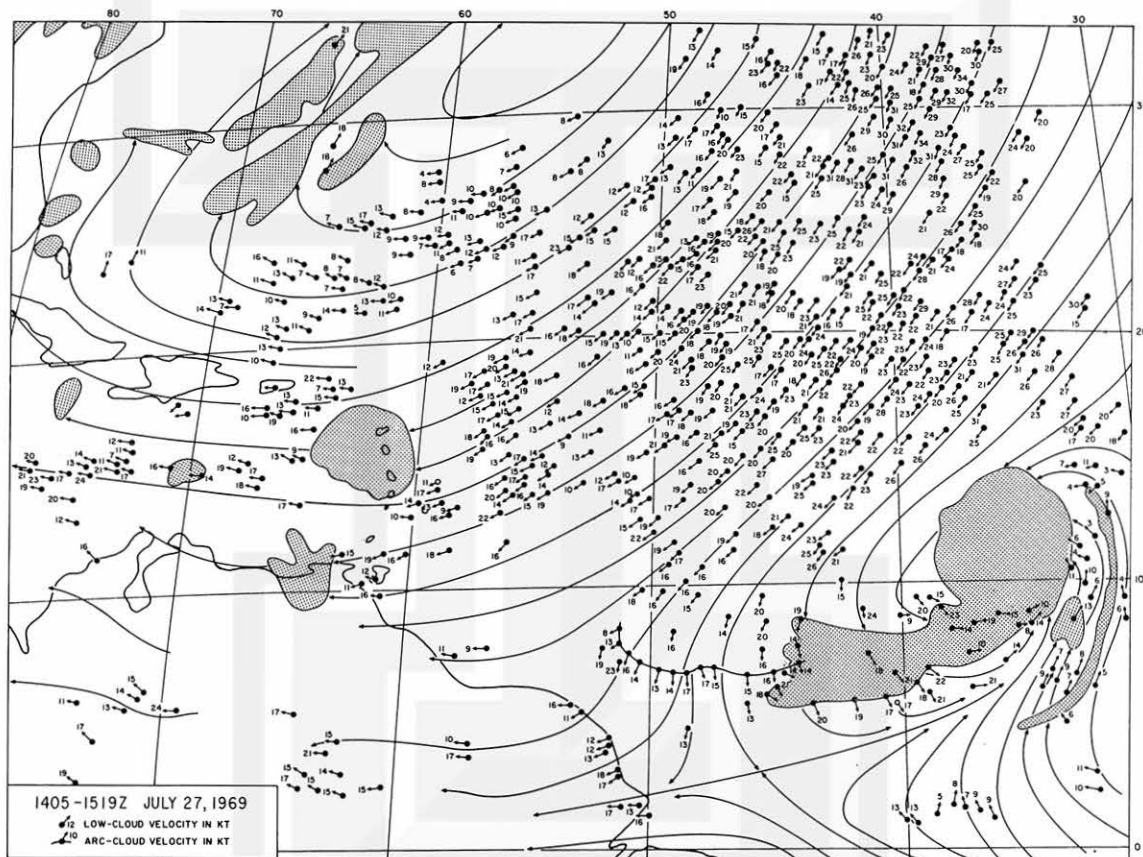


Fig. 4. Velocity vectors of low clouds for the analysis area in Fig. 2 on July 27, 1969 with superimposed streamlines. High clouds, shown as shaded areas, associated with storm Anna are on the lower right section. (From Chang and Tecson, 1974.)

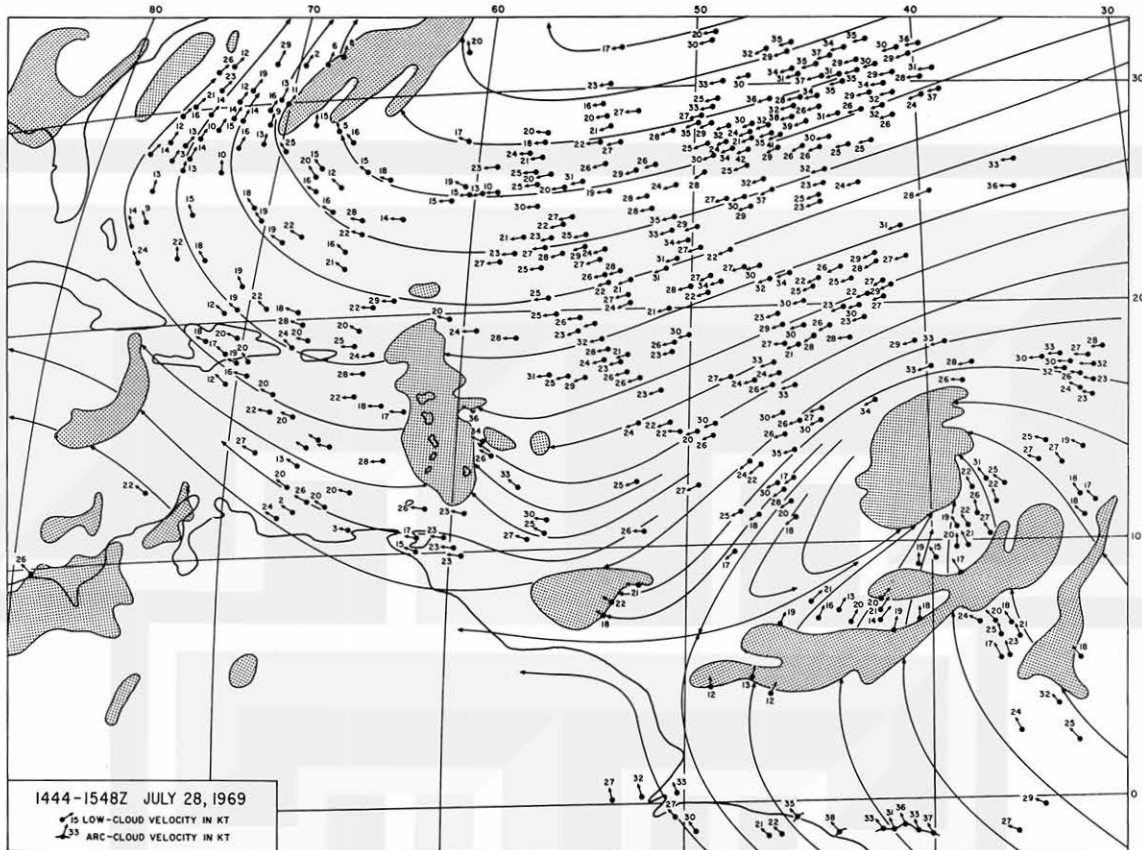


Fig. 5. Velocity vectors of low clouds for the analysis area in Fig. 2 on July 28, 1969 with superimposed streamlines. High clouds, shown as shaded areas, associated with storm Anna are on the lower right section. (From Chang and Tecson, 1974.)

characteristics inherent in the streamline-isotach analysis. The storm is sectorized into two or three areas according to the dominant flow pattern as shown in Fig. 6. The sectors, as defined by the dashed lines, are classified as the northern sector (○), the western sector (□), and the southern sector (●). The number of vectors corresponding to each sector is indicated; the total number for each day is entered in the lower right portion of the chart. The significant cloud boundaries associated with the storm are likewise shown. With the center of the storm as origin, a circle of radius 10.5 latitude is circumscribed; this encloses the region of computation. The unshaded portion at the right edge of the circle defines the area where cloud vectors are not obtained, this being beyond the coverage of the movie loop.

JULY 1969

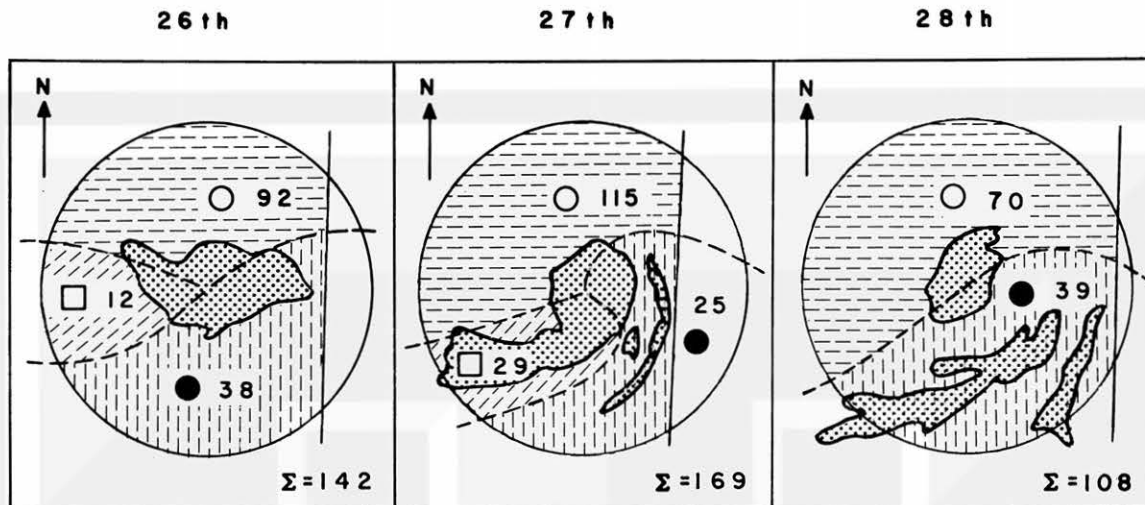


Fig. 6. Tropical storm Anna divided into sectors, within 10.5 degree-latitude radius from the center. They are identified as the northern sector (○), the western sector (□), and the southern sector (●). The number of the respective cloud vectors and the total for each day are shown. Unshaded portion of circle shows area where cloud vectors are not obtained.

The radial and tangential components are averaged for every degree of latitude distance for each sector. By observing the non-uniformity of the distribution of the vectors around the center, it is not expected to bring out equal sample sizes for each partition. Nevertheless, simple averaging is done for each degree radius. Whenever a sample point occurs at the boundaries, it is counted on both sides of the adjacent areas to be averaged.

#### 4. SOURCES OF ERROR

The accuracy of the results of the analyses discussed in this paper depends on the errors contributed by the various factors which merit enumeration. Fujita *et al.* (1973) have estimated that the tracking error generated by the METRACOM system for calculating cloud velocities appear to vary within 1 m/sec. Cloud directions could vary by about 5 degrees. The manual tracking of clouds is considered quite proficient enough that errors are sufficiently minimized through meteorological expertise of the particular

flow patterns involved and with more experience. It is also highly possible that the low-cloud motion levels analyzed may not always be the same for different days since inflow levels could have varied as the storm intensity changes. This could well be a factor in attempting to establish definite relationships between cloud flow and wind flow.

As could be noticed in Fig. 6, and particularly on July 27, certain areas in the northern and southern sectors of the storm beyond the radial distance of 6 degrees are devoid of data since, unfortunately, they fall beyond the area of the movie loop. The effect on the northern sector may not be felt since the missing area is rather small and there are sufficient vectors already. How it may affect the data distribution on the southern sector of the storm could only be surmised, although it is believed not to be of critical extent. Examination of the results of the analyses of July 27 tend to show that, while more vectors would stabilize the data, its behavior, compared on a day-by-day basis for the same sector, may not be significantly different from the present results. The effect of additional data, if at all, on both components would most probably be towards increasing the inflow and circulation around the storm; it would lead to better conclusions. In spite of the potential increase in the data points for July 27 and, to a lesser extent, for July 26, it should be noted that the present sample size for these days are already much more than those for July 28 where almost the whole storm area is trackable. Adding a few more vectors for the southern sector for July 27 would certainly be advantageous although, comparatively, it already has 2/3rds of the number observed for the same vector for the other days.

## 5. RESULTS OF ANALYSES

### a. Mean Radial Velocities

Figure 7 shows the scatter diagrams of the radial velocities of tropical storm Anna for July 26, 27 and 28, 1969 from its center extending a little beyond the radial distance of 10 degrees. The observations are plotted in appropriate symbols according to the various sectors in which they have been classified. Corresponding mean values for every degree-latitude radial distance are plotted and drawn proportional to the frequency of observation and joined by a solid straight line. Where broken lines appear, they indicate absence of mean value in the particular area. It should be noted, however, that when only one observation occurs within its 1-degree boundary at either extremity

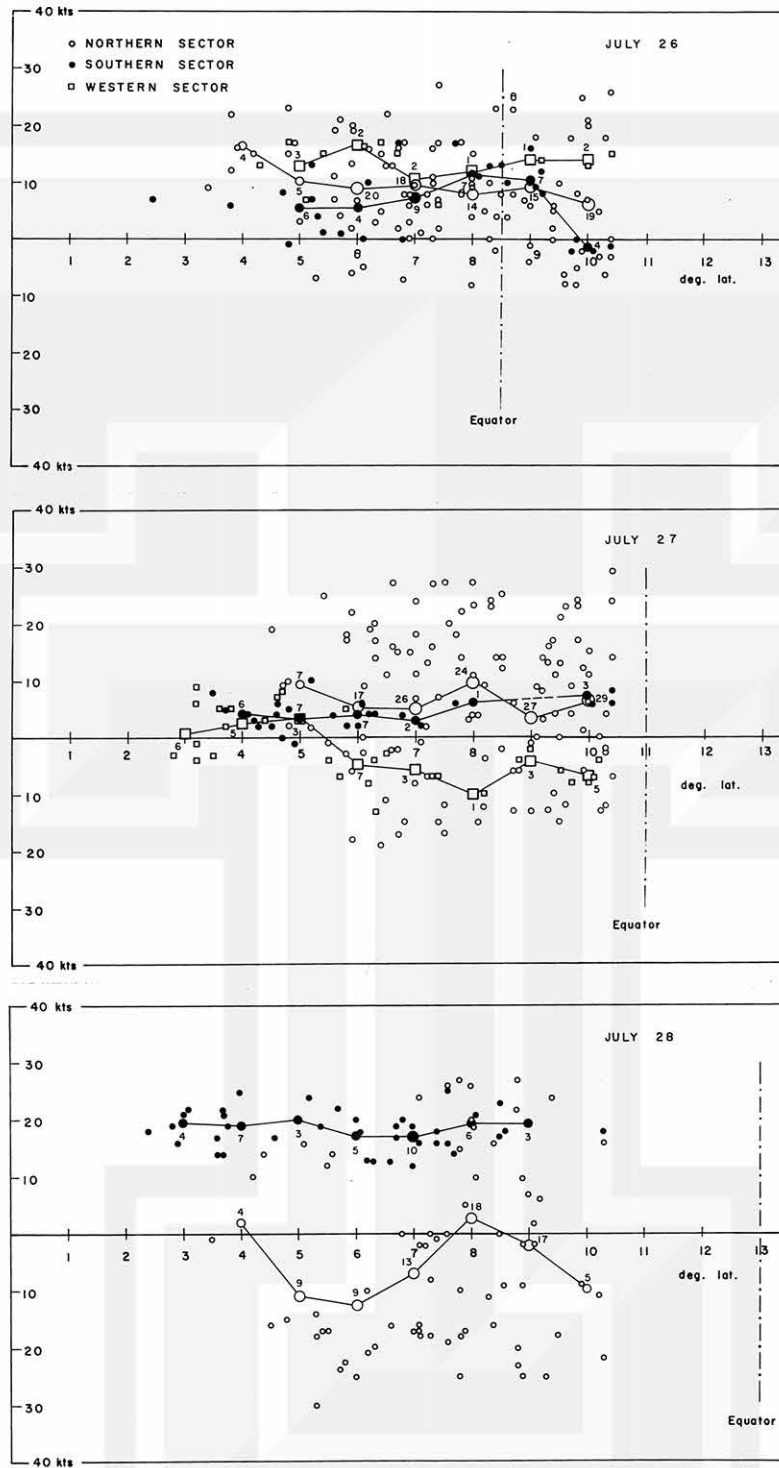


Fig. 7. Scatter diagrams of the radial low-cloud velocities of tropical storm Anna, by sector, for July 26, 27 and 28, 1969. Corresponding mean values, with frequencies indicated, are connected by a line. Distance of the equator from the circulation center is also shown.

of the radial distance range, no mean value is computed. No mean-value symbol and line, therefore, are drawn at these ends.

The northern sector shows a daily decrease in radial velocity inflow as the storm progresses. During July 26 and 27, it has inflow at all radii. On the 28th, it shows outflow at all areas except at the 8-degree radius; it averages 5 kts. The western sector exhibits a varying degree of inflow on the 26th. The following day, its inflow has decreased and, beyond the 5-degree radius, it has shown outflow characteristics. On July 28, its flow has turned southerly, thus merging with the southern sector. On the other hand, the southern sector shows a slight decrease in inflow from July 26, when it averaged 6 kts, to July 27, when it averaged 5 kts. But suddenly on the 28th, after Anna has attained storm intensity, it indicated a marked increase and a constant inflow at all radii of about 20 kts. This suggests that the cross-equatorial flow from the southern hemisphere, which predominates in the southern sector of the storm, is apparently the major contributor to the inflow as tropical storm Anna intensified.

#### b. Mean Tangential Velocities

Presented in Fig. 8 are the scatter diagrams of the tangential velocities of tropical storm Anna for July 26, 27 and 28, 1969. The manner of plotting and representation are the same as that in the previous figure.

On the whole, there does not appear to be a drastic change in the intensity characteristics for the northern sector of the storm during these three days. It remains relatively high. On July 26 and 28, the average tangential velocity for all plotted radii are well close to 20 kts. There is a slight decrease on the 27th by about 2 kts. For the western sector, the average tangential velocity of about 14 kts appears to increase by a small amount from July 26 to 27. It is rather difficult to generalize the daily trend for the southern sector of the storm for the whole period, although it can roughly be summarized that the circulation has changed from anticyclonic on July 26 to cyclonic from July 27 through 28. It might also be noticed that if the various sectors are compared during the 3-day period, the weakest contribution to the tangential velocity field is the southern sector, while the strongest is the northern sector. It appears from this relationship, therefore, that the circulation around the storm is mostly achieved at the northern portion where the northern hemisphere trades prevail. Contri-

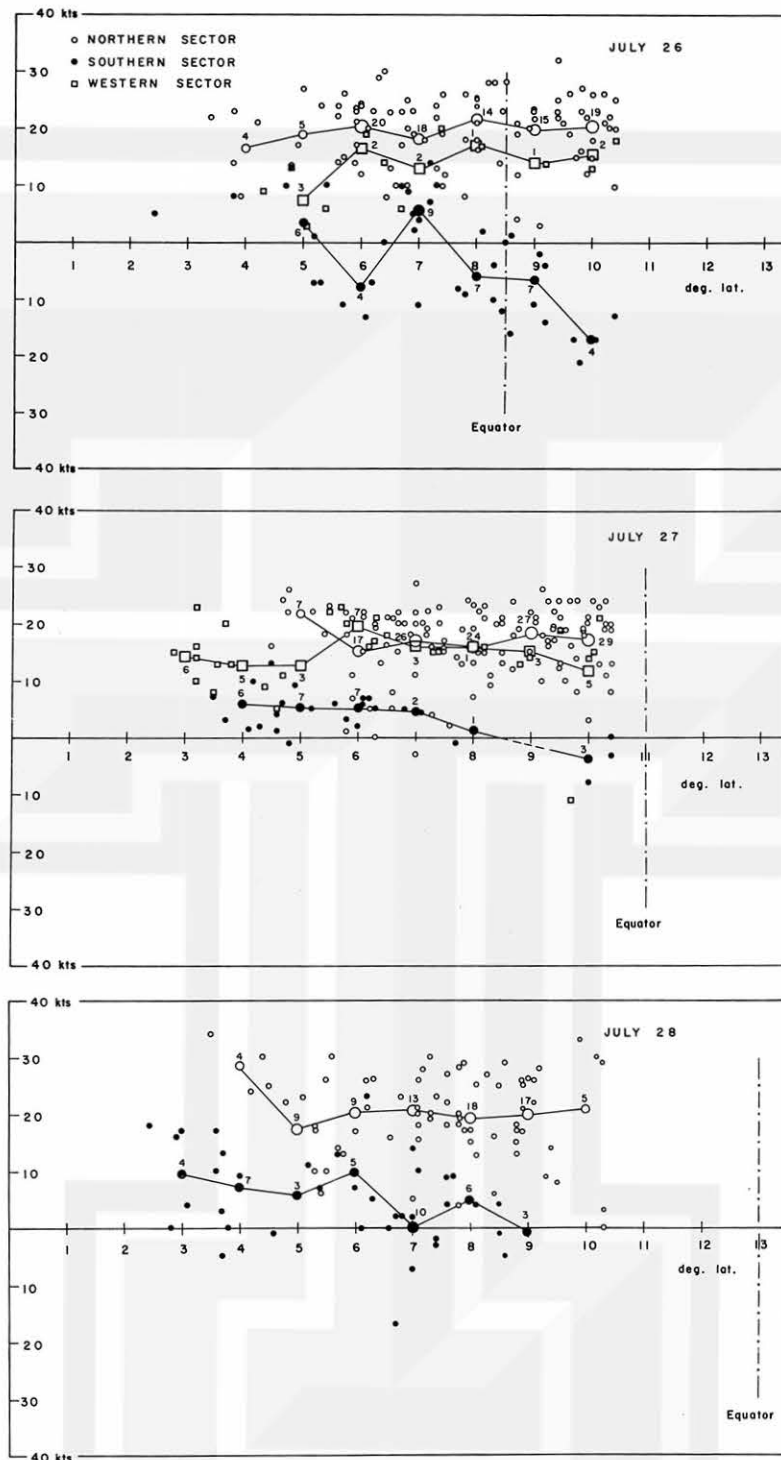


Fig. 8. Scatter diagrams of the tangential low-cloud velocities of tropical storm Anna, by sector, for July 26, 27 and 28, 1969. Corresponding mean values, with frequencies indicated, are connected by a line. Distance of the equator from the circulation center is also shown.

butions by the western and southern sectors, though by smaller amounts, are toward increasing cyclonic circulation as the storm intensifies. Commenting on the general characteristics of the various sectors during the period, taking into account both mean radial and tangential velocities, it may be inferred from Table 1 that the most consistent contributor toward storm intensification is the southern sector of the storm which shows increased inflow by a considerable amount and also increased circulation, though by a comparatively smaller amount.

Table 1. Circulation and Inflow Characteristics for the Low-Cloud Velocities for Tropical Storm Anna, July 26 through 28, 1969.

Sector	Inflow	Circulation
Northern	Decrease	Increase
Western	Decrease	Increase
Southern	Increase	Increase

The distribution of the radial and tangential velocities of the low clouds in Figs. 7 and 8 indicate that there are only a few vectors plotted within the first 3 degrees of radial distance from the storm center. This is due to the scarcity of reliable cloud tracer points within the area. Since the characteristic large-cloud mass dominates the central storm system, unfortunately, satellite photographs show some degree of brightness saturation in this region. Picture enhancements could yield better results, however.

#### c. Mean Divergence

The mean horizontal velocity divergence in a region may be expressed as

$$\text{div}_H = -\frac{1}{A} \oint V_R dS$$

where  $A$  is the area over which the divergence is measured and  $V_R$  is the velocity component normal to the distance  $S$  extending along the boundary of  $A$  and defined positive inwards. The mean divergence profile for storm Anna for the three days for each sector is shown in Fig. 9. Mean low-cloud velocity for each degree distance is

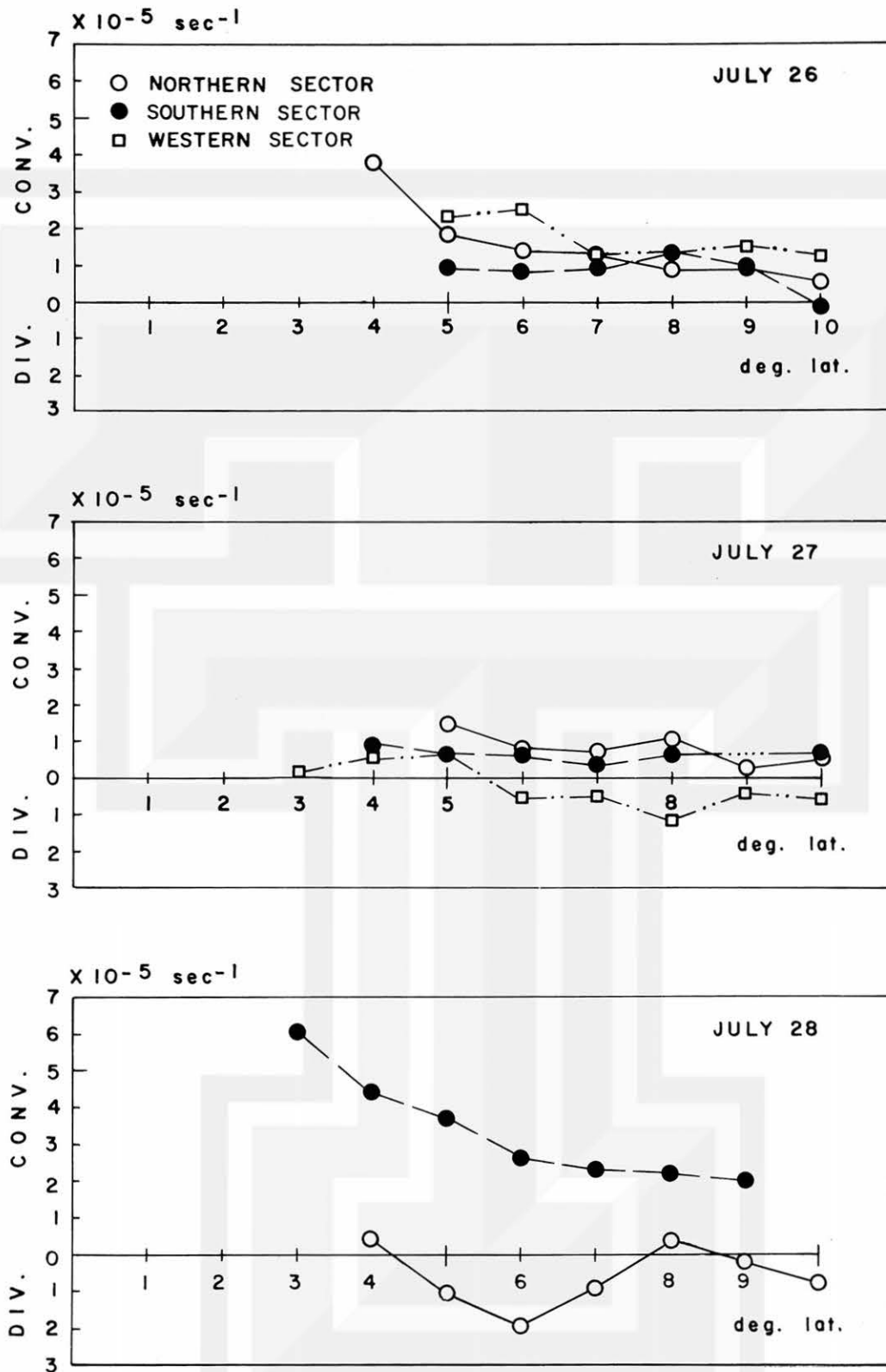


Fig. 9. Mean divergence profile of tropical storm Anna, by sector, for July 26, 27 and 28, 1969 using low-cloud velocities. No symbol appears whenever a mean value is not calculated.

used. Most noticeable is the increasing influence of the southern sector of the storm as Anna intensifies. Note the absence of data within the inner radius of the storm in this and the next two figures.

#### d. Mean Relative Vorticity

The mean relative vorticity ( $\zeta_r$ ) of a region may be computed from the expression

$$\zeta_r = \frac{1}{A} \oint V_T dS$$

where  $V_T$  is the velocity component parallel to the distance  $S$  extending along the boundary of  $A$  and defined positive cyclonically. Also using mean low-cloud velocities, the mean relative vorticity profile is shown in Fig. 10. Computations are made for the same area as, and in a manner similar to, Fig. 9. The major influence of the northern sector of the storm may be seen clearly as the storm intensifies. To a lesser extent, the southern portion also exerts increasing cyclonic motion to the storm.

#### e. Mean Absolute Angular Momentum

The mean absolute angular momentum for the low-cloud level determined for the various sectors for the 3-day period from July 26 through 28, 1969 are shown in Fig. 11. When expressed in a cylindrical coordinate system with the origin at the storm center, it is computed from the expression

$$M = V_T R + \frac{fR^2}{2}$$

where  $V_T$  is the mean tangential velocity,  $R$  is the radial distance from the center and  $f$  is a variable Coriolis parameter. Since the tangential component of the cloud motion vector is involved, its distribution in the northern sector of the storm is discussed. It is seen that the absolute angular momentum decreases as the radial distance from the center diminishes. This is a natural consequence for winds, and similarly for cloud motions, to lose absolute angular momentum as they travel from the outermost areas and spiral inward toward the storm center. Table 2 shows the radial distribution for the northern sector broken down into its two components. Com-

Table 2. Radial Distribution of Mean Absolute Angular Momentum  
for Low-Cloud Motions for the Northern Sector of Storm Anna  
( $\times 10^6 \text{ m}^2 \text{ sec}^{-1}$ )

Radius ( $^{\circ}$ Latitude)	2	3	4	5	6	7	8	9	10
<u>July 26, 1969</u>									
$V_T R$	*	*	3.8	5.4	7.0	7.3	9.9	10.2	11.5
$\frac{1}{2}fR^2$	*	*	2.9	4.9	7.5	10.9	15.0	20.0	25.9
M	*	*	6.7	10.3	14.5	18.2	24.9	30.2	37.4
<u>July 27, 1969</u>									
$V_T R$	*	*	*	6.2	5.1	6.7	7.4	9.5	9.8
$\frac{1}{2}fR^2$	*	*	*	6.0	8.4	12.4	17.3	22.0	37.3
M	*	*	*	12.2	13.5	19.1	24.7	31.5	47.1
<u>July 28, 1969</u>									
$V_T R$	*	*	6.5	5.0	7.0	8.2	8.8	10.2	11.8
$\frac{1}{2}fR^2$	*	*	4.0	5.7	8.6	13.0	17.0	23.0	29.0
M	*	*	10.5	10.7	15.6	21.2	25.8	33.2	40.8

\* No computation due to lack of data

paring July 26 and 28, for all radii, there is an increase in momentum values. The same observation holds for July 27 and 28, except for the 5- and 10-degree radius. On the whole, an increase in momentum is evident in the 3-day period. The contribution of the term containing the Coriolis parameter becomes predominant beyond the 5- or 6-degree distance from the center. The same feature is noted in the computation of the absolute angular momentum of a typhoon circulation from displacement vectors of small radar echoes by Fujita et al. (1966).

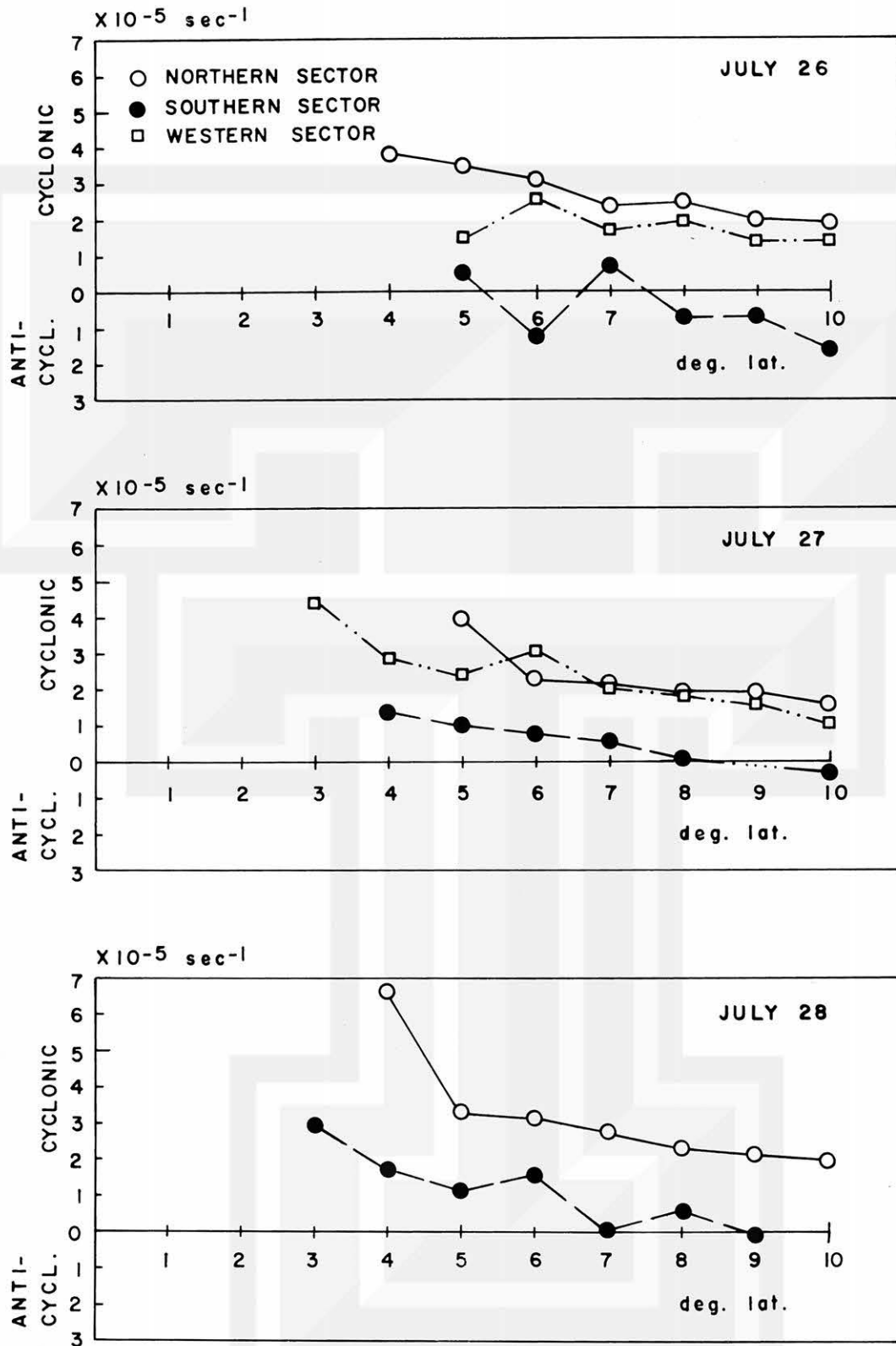


Fig. 10. Mean relative vorticity profile of tropical storm Anna, by sector, for July 26, 27 and 28, 1969 using low-cloud velocities. No symbol appears whenever a mean value is not calculated.

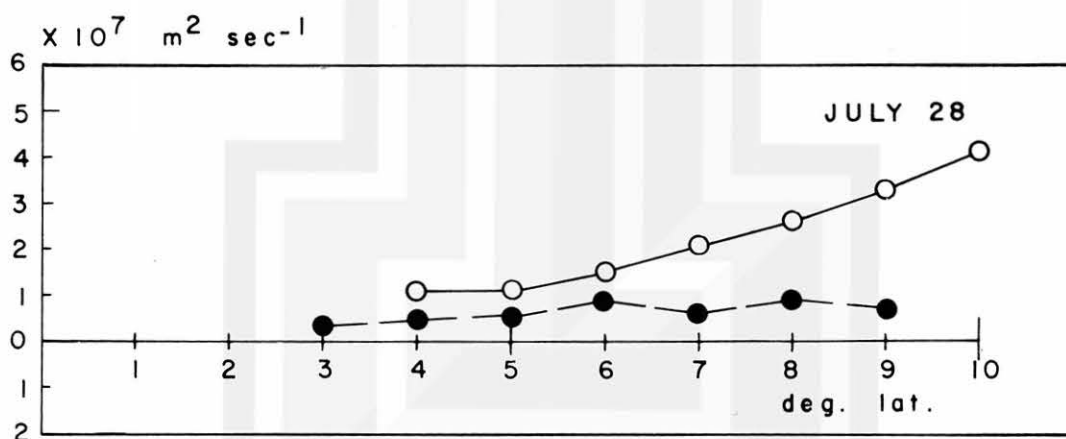
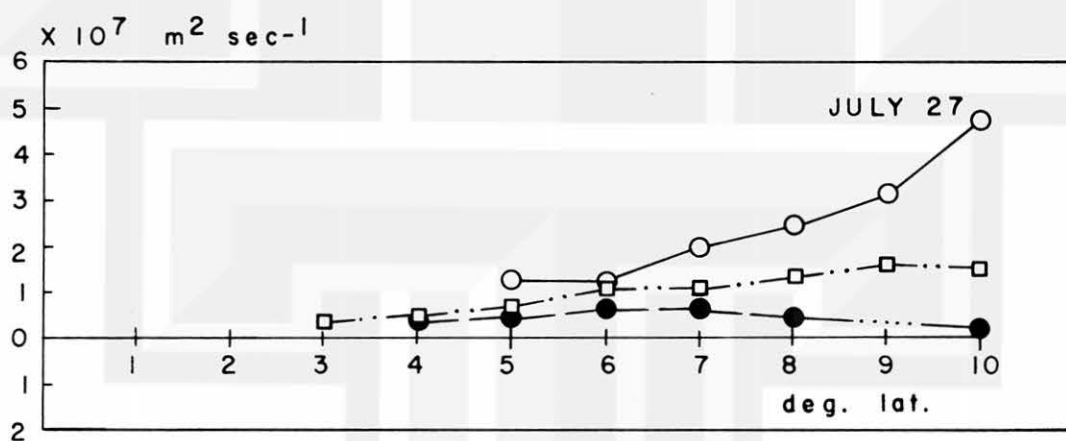
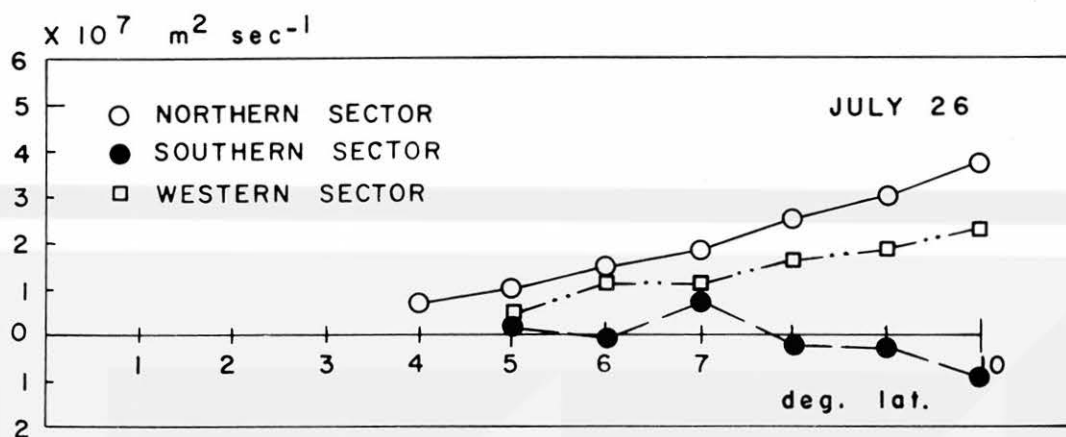


Fig. 11. Radial distribution of the mean absolute angular momentum for the low-cloud level of tropical storm Anna, by sector, for July 26, 27 and 28, 1969. No symbol appears whenever a mean value is not calculated.

## 6. CONCLUSIONS

A kinematic analysis of tropical storm Anna within a 10-degree latitude radial distance from its center during the three days on July 26 to 28, 1969 has been made using computed low-cloud velocities from ATS pictures. Anna's intensification into a tropical storm over the North Atlantic Ocean was reported to have occurred late on the 27th. The asymmetric structure of the storm has been maintained by using the total cloud velocities. The storm is divided initially into three sectors, each of which has been individually analyzed. Unfortunately, few data available within the inner radius of the disturbance preclude evaluation near the center.

Examination of the overall increase in tangential velocities reflects storm intensification as time progresses. What has been anticyclonic circulation at the beginning date has later become cyclonic flow. The increase, in time, also of the radial components is most conspicuous in the southern sector of the storm, and especially in the horizontal divergence computations. Considering both the radial and tangential velocities for each sector of the storm during the 3-day period, it is observed that the most consistent contributor toward storm intensification is the southern sector which has exhibited increase in both inflow and cyclonic circulation. Likewise, the relative vorticity patterns show increase during the period. The mean absolute angular momentum computations indicate the loss of momentum as the cloud particles moving from the outer radius spiral toward the storm center. It is observed that the contribution of the term containing the Coriolis parameter becomes greater than the velocity term beyond the 5- or 6-degree distance from the storm center.

Results of the analyses for this storm strongly show that the cross-equatorial flow from the southern hemisphere is mainly responsible for providing the inflow to the storm while the northern hemisphere trades supply the major contribution to the circulation around this storm.



## REFERENCES

- Agee, E. M. , 1972: Note on ITCZ Wave Disturbances and Formation of Tropical Storm Anna. Monthly Weather Review, Vol. 100, No. 10, pp. 733-737.
- Chang, Y. M. , J. J. Tecson and T. T. Fujita, 1973: METRACOM System of Cloud Velocity Determination from Geostationary Satellite Pictures. SMRP Research Paper 110, The University of Chicago.
- \_\_\_\_\_ and J. J. Tecson, 1974: Cloud Velocities over the North Atlantic Computed from ATS Picture Sequences. SMRP Research Paper 121, The University of Chicago.
- De Angelis, R. M. , 1970: North Atlantic Tropical Cyclones. Climatological Data, National Summary, Annual 1969, ESSA 20, No. 13, pp. 60-68.
- Fujita, T. , T. Izawa, K. Watanabe and I. Imai, 1966: A Model of Typhoons Accompanied by Inner and Outer Rainbands. SMRP Research Paper 60, The University of Chicago.
- \_\_\_\_\_ D. L. Bradbury, C. Murino and L. Hull, 1968: A Study of Mesoscale Cloud Motions Computed from ATS-I and Terrestrial Photographs. SMRP Research Paper 71, The University of Chicago.
- \_\_\_\_\_, E. W. Pearl and W. E. Shenk, 1973: Satellite-Tracked Cloud Velocities. SMRP Research Paper 114, The University of Chicago.
- Serebreny, S. , W. E. Evans, R. G. Hadfield and E. J. Wiegman, 1967: Detection of Cloud Displacement Using Video Techniques. Stanford Research Institute, Menlo Park, California, 37 pp.
- Suomi, V. E. , et al. , 1972: McIDAS, Man-Computer Interaction Data Access System. Space Science and Engineering Center, University of Wisconsin at Madison, 39 pp.

MESOMETEOROLOGY PROJECT - - - RESEARCH PAPERS

(Continued from front cover)

42. \* A Study of Factors Contributing to Dissipation of Energy in a Developing Cumulonimbus - Rodger A. Brown and Tetsuya Fujita
43. A Program for Computer Gridding of Satellite Photographs for Mesoscale Research - William D. Bonner
44. Comparison of Grassland Surface Temperatures Measured by TIROS VII and Airborne Radiometers under Clear Sky and Cirriform Cloud Conditions - Ronald M. Reap
45. Death Valley Temperature Analysis Utilizing Nimbus I Infrared Data and Ground-Based Measurements - Ronald M. Reap and Tetsuya Fujita
46. On the "Thunderstorm-High Controversy" - Rodger A. Brown
47. Application of Precise Fujita Method on Nimbus I Photo Gridding - Lt. Cmd. Ruben Nasta
48. A Proposed Method of Estimating Cloud-top Temperature, Cloud Cover, and Emissivity and Whiteness of Clouds from Short- and Long-wave Radiation Data Obtained by TIROS Scanning Radiometers - T. Fujita and H. Grandoso
49. Aerial Survey of the Palm Sunday Tornadoes of April 11, 1965 - Tetsuya Fujita
50. Early Stage of Tornado Development as Revealed by Satellite Photographs - Tetsuya Fujita
51. Features and Motions of Radar Echoes on Palm Sunday, 1965 - D. L. Bradbury and T. Fujita
52. Stability and Differential Advection Associated with Tornado Development - Tetsuya Fujita and Dorothy L. Bradbury
53. Estimated Wind Speeds of the Palm Sunday Tornadoes - Tetsuya Fujita
54. On the Determination of Exchange Coefficients: Part II - Rotating and Nonrotating Convective Currents - Rodger A. Brown
55. Satellite Meteorological Study of Evaporation and Cloud Formation over the Western Pacific under the Influence of the Winter Monsoon - K. Tsuchiya and T. Fujita
56. A Proposed Mechanism of Snowstorm Mesojet over Japan under the Influence of the Winter Monsoon - T. Fujita and K. Tsuchiya
57. Some Effects of Lake Michigan upon Squall Lines and Summertime Convection - Walter A. Lyons
58. Angular Dependence of Reflection from Stratiform Clouds as Measured by TIROS IV Scanning Radiometers - A. Rabbe
59. Use of Wet-beam Doppler Winds in the Determination of the Vertical Velocity of Raindrops inside Hurricane Rainbands - T. Fujita, P. Black and A. Loesch
60. A Model of Typhoons Accompanied by Inner and Outer Rainbands - Tetsuya Fujita, Tatsuo Izawa, Kazuo Watanabe and Ichiro Imai
61. Three-Dimensional Growth Characteristics of an Orographic Thunderstorm System - Rodger A. Brown
62. Split of a Thunderstorm into Anticyclonic and Cyclonic Storms and their Motion as Determined from Numerical Model Experiments - Tetsuya Fujita and Hector Grandoso
63. Preliminary Investigation of Peripheral Subsidence Associated with Hurricane Outflow - Ronald M. Reap
64. The Time Change of Cloud Features in Hurricane Anna, 1961, from the Easterly Wave Stage to Hurricane Dissipation - James E. Arnold
65. Easterly Wave Activity over Africa and in the Atlantic with a Note on the Intertropical Convergence Zone during Early July 1961 - James E. Arnold
66. Mesoscale Motions in Oceanic Stratus as Revealed by Satellite Data - Walter A. Lyons and Tetsuya Fujita
67. Mesoscale Aspects of Orographic Influences on Flow and Precipitation Patterns - Tetsuya Fujita
68. A Mesometeorological Study of a Subtropical Mesocyclone -Hidetoshi Arakawa, Kazuo Watanabe, Kiyoshi Tsuchiya and Tetsuya Fujita
69. Estimation of Tornado Wind Speed from Characteristic Ground Marks - Tetsuya Fujita, Dorothy L. Bradbury and Peter G. Black
70. Computation of Height and Velocity of Clouds from Dual, Whole-Sky, Time-Lapse Picture Sequences - Dorothy L. Bradbury and Tetsuya Fujita
71. A Study of Mesoscale Cloud Motions Computed from ATS-I and Terrestrial Photographs - Tetsuya Fujita, Dorothy L. Bradbury, Clifford Murino and Louis Hull
72. Aerial Measurement of Radiation Temperatures over Mt. Fuji and Tokyo Areas and Their Application to the Determination of Ground- and Water-Surface Temperatures - Tetsuya Fujita, Gisela Baralt and Kiyoshi Tsuchiya
73. Angular Dependence of Reflected Solar Radiation from Sahara Measured by TIROS VII in a Torquing Maneuver - Rene Mendez.
74. The Control of Summertime Cumuli and Thunderstorms by Lake Michigan During Non-Lake Breeze Conditions - Walter A. Lyons and John W. Wilson
75. Heavy Snow in the Chicago Area as Revealed by Satellite Pictures - James Bunting and Donna Lamb
76. A Model of Typhoons with Outflow and Subsidence Layers - Tatsuo Izawa

\* out of print

(continued on outside back cover)

SATELLITE AND MESOMETEOROLOGY RESEARCH PROJECT --- PAPERS

77. Yaw Corrections for Accurate Gridding of Nimbus HRIR Data - R. A. Madden
78. Formation and Structure of Equatorial Anticyclones caused by Large-Scale Cross Equatorial Flows determined by ATS I Photographs - T. T. Fujita, K. Watanabe and T. Izawa
79. Determination of Mass Outflow from a Thunderstorm Complex using ATS III Pictures - T. T. Fujita and D. L. Bradbury
80. Development of a Dry Line as shown by ATS Cloud Photography and verified by Radar and Conventional Aerological Data - D. L. Bradbury
81. Dynamical Analysis of Outflow from Tornado-Producing Thunderstorms as revealed by ATS III Pictures - K. Ninomiya
- \*82. Computation of Cloud Heights from Shadow Positions through Single Image Photogrammetry of Apollo Pictures - T. T. Fujita
83. Aircraft, Spacecraft, Satellite and Radar Observations of Hurricane Gladys, 1968 - R. C. Gentry, T. Fujita and R. C. Sheets
84. Basic Problems on Cloud Identification related to the design of SMS-GOES Spin Scan Radiometers - T. T. Fujita
85. Mesoscale Modification of Synoptic Situations over the Area of Thunderstorms' Development as revealed by ATS III and Aerological Data - K. Ninomiya
86. Palm Sunday Tornadoes of April 11, 1965 - T. T. Fujita, D. L. Bradbury and C. F. Van Thullenar  
(Reprinted from Mon. Wea. Rev., 98, 29-69, 1970)
87. Patterns of Equivalent Blackbody Temperature and Reflectance of Model Clouds computed by changing Radiometer's Field of View - J. J. Tecson
88. Lubbock Tornadoes of 11 May 1970 - T. T. Fujita
89. Estimate of Areal Probability of Tornadoes from Inflationary Reporting of their Frequencies - T. T. Fujita
90. Application of ATS III Photographs for determination of Dust and Cloud Velocities over Northern Tropical Atlantic - T. T. Fujita
91. A Proposed Characterization of Tornadoes and Hurricanes by Area and Intensity - T. T. Fujita
92. Estimate of Maximum Wind Speeds of Tornadoes in Three Northwestern States - T. T. Fujita
93. In- and Outflow Field of Hurricane Debbie as revealed by Echo and Cloud Velocities from Airborne Radar and ATS-III Pictures - T. T. Fujita and P. G. Black (Reprinted from Preprint of Radar Meteorology Conference, Nov. 17-20, 1970, Tucson, Arizona)
94. Characterization of 1965 Tornadoes by their Area and Intensity - J. J. Tecson
- \*95. Computation of Height and Velocity of Clouds over Barbados from a Whole-Sky Camera Network - R. D. Lyons
96. The Filling over Land of Hurricane Camille, August 17-18, 1969 - D. L. Bradbury
97. Tornado Occurrences related to Overshooting Cloud-Top Heights as determined from ATS Pictures - T. T. Fujita
98. FPP Tornado Scale and its Applications - T. T. Fujita and A. D. Pearson
99. Preliminary Results of Tornado Watch Experiment 1971 - T. T. Fujita, J. J. Tecson and L. A. Schaal
100. F-Scale Classification of 1971 Tornadoes - T. T. Fujita
101. Typhoon-Associated Tornadoes in Japan and new evidence of Suction Vortices in a Tornado near Tokyo - T. T. Fujita
102. Proposed Mechanism of Suction Spots accompanied by Tornadoes - T. T. Fujita
103. A Climatological Study of Cloud Formation over the Atlantic during Winter Monsoon - H. Shitara
- \*\*104. Statistical Analysis of 1971 Tornadoes - E. W. Pearl
105. Estimate of Maximum Windspeeds of Tornadoes in Southernmost Rockies - T. T. Fujita
106. Use of ATS Pictures in Hurricane Modification - T. T. Fujita
107. Mesoscale Analysis of Tropical Latin America - T. T. Fujita
108. Tornadoes Around The World - T. T. Fujita (Reprinted from Weatherwise, 26, No. 2, April 1973)
109. A Study of Satellite-Observed Cloud Patterns of Tropical Cyclones - E. E. Balogun
110. METRACOM System of Cloud-Velocity determination from Geostationary Satellite Pictures - Y. M. Chang, J. J. Tecson and T. T. Fujita
111. Proposed Mechanism of Tornado Formation from Rotating Thunderstorm - T. T. Fujita
112. Joliet Tornado of April 6, 1972 - E. W. Pearl
113. Results of FPP Classification of 1971 and 1972 Tornadoes - T. T. Fujita and A. D. Pearson
114. Satellite-Tracked Cumulus Velocities - T. T. Fujita, E. W. Pearl and W. E. Shenk
115. General and Local Circulation of Mantle and Atmosphere toward Prediction of Earthquakes and Tornadoes - T. T. Fujita and K. Fujita
116. Cloud Motion Field of Hurricane Ginger during the Seeding Period as determined by the METRACOM System - J. J. Tecson, Y. M. Chang and T. T. Fujita
117. Overshooting Thunderheads observed from ATS and Learjet - T. T. Fujita
118. Thermal and Dynamical Features of a Thunderstorm with a Tilted Axis of Rotation - T. T. Fujita
119. Characteristics of Anvil-Top Associated with the Poplar Bluff Tornado of May 7, 1973 - E. W. Pearl
120. Jumbo Tornado Outbreak of 3 April 1974 - T. T. Fujita
121. Cloud Velocities Over The North Atlantic Computed From ATS Picture Sequences - Y. M. Chang and J. J. Tecson
122. Analysis of Anvil Growth For ATS Pictures - Y. M. Chang
123. Evaluation of Tornado Risk Based On F-Scale Distribution - E. W. Pearl
124. Superoutbreak Tornadoes Of April 3, 1974 As Seen In ATS Pictures - T. T. Fujita and G. S. Forbes